Accepted Manuscript

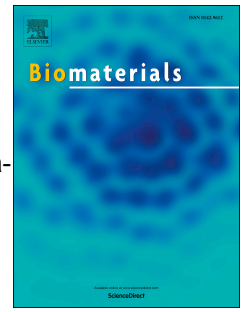

Glucose & oxygen exhausting liposomes for combined cancer starvation and hypoxia-activated therapy

Rui Zhang, Liangzhu Feng, Ziliang Dong, Li Wang, Chao Liang, Jiawen Chen, Qingxi Ma, Rui Zhang, Qian Chen, Yucai Wang, Zhuang Liu

PII: S0142-9612(18)30084-X

DOI: 10.1016/j.biomaterials.2018.02.004

Reference: JBMT 18477

To appear in: *Biomaterials*

Received Date: 14 November 2017

Revised Date: 8 January 2018

Accepted Date: 2 February 2018

Please cite this article as: Zhang R, Feng L, Dong Z, Wang L, Liang C, Chen J, Ma Q, Zhang R, Chen Q, Wang Y, Liu Z, Glucose & oxygen exhausting liposomes for combined cancer starvation and hypoxia-activated therapy, *Biomaterials* (2018), doi: 10.1016/j.biomaterials.2018.02.004.

Glucose & Oxygen Exhausting Liposomes for Combined Cancer Starvation and Hypoxia-Activated Therapy

Rui Zhang[†], Liangzhu Feng[†]*, Ziliang Dong[†], Li Wang[‡], Chao Liang[†], Jiawen Chen[†], Qingxi Ma[†], Rui Zhang[†], Qian Chen[†], Yucai Wang[‡], Zhuang Liu[†]*

[†] Institute of Functional Nano & Soft Materials (FUNSOM), Jiangsu Key Laboratory for Carbon-Based Functional Materials & Devices, Soochow University, Suzhou 215123, China.

[‡]The CAS Key Laboratory of Innate Immunity and Chronic Diseases, School of Life Sciences and Medical Center, the University of Science & Technology of China, Hefei, Anhui 230027, China.

E-mail: zliu@suda.edu.cn, lzfeng@suda.edu.cn

Keywords: AQ4N, glucose oxidase, liposome, starvation therapy, tumor hypoxia-activated therapy

Abstract: Starvation therapy to slow down the tumor growth by cutting off its energy supply has been proposed to be an alternative therapeutic strategy for cancer treatment. Herein, glucose oxidase (GOx) is loaded into stealth liposomes and act as the glucose and oxygen elimination agent to trigger the conversion of glucose and oxygen into gluconic acid and H_2O_2. Such liposome-GOx after intravenous injection with effective tumor retention is able to exhaust glucose and oxygen within the tumor, producing cytotoxic H_2O_2 and enhancing hypoxia, as vividly visualized by non-invasive *in vivo* photoacoustic imaging. By further combination treatment with stealth liposomes loaded with banoxantrone dihydrochloride (AQ4N), a hypoxia-activated pro-drug, a synergistically enhanced tumor growth inhibition effect is achieved in the mouse model of 4T1 tumor. Hence, by combining starvation therapy and hypoxia-activated therapy tactfully utilizing liposomal nanocarriers to co-deliver both enzymes and prodrugs, an innovative strategy is presented in this study for effective cancer treatment.

1. Introduction

Recently, cancer metabolism, particularly glucose metabolism, has received growing interests in the design of cancer therapy, such as reprogramming or hindering energy supply pathway for cancer cells [1-6]. Based on the Warburg effect, proliferating cancer cells would consume much more glucose than normal tissues to produce energy [4, 7, 8]. Therefore, some alternative cancer treatment strategies have been proposed to impede the glucose consumption such as glucose transporter inhibitors [3, 9]. As the blockade of glucose supply can only slow down the tumor growth without complete cancer cell killing, the combination of this strategy with other therapeutic approaches may be an attractive choice [10-12].

Tumor hypoxia, mainly resulting from rapid tumor growth induced inefficient microvascular systems, is a common characteristic of most solid tumors which has been found to hinder treatment outcomes for many types of cancer therapeutics [13-16]. Therefore, various strategies have been implemented to overcome these obstacles of tumor hypoxia to improve prognosis. For instance, relieving tumor hypoxia by increasing tumor oxygen supply has been demonstrated to be beneficial to improve the therapeutic efficacies of different types of therapies [17-24]. On the other hand, hypoxia-activated prodrugs, which are activated by reducing enzymes under hypoxic tumor regions and show minimized systemic side effects to normal tissues with normoxia, have gained extensive interests both in basic research and clinical trials [25-28]. Moreover, hypoxia-activated prodrugs may be combined with other types of therapeutics such as oxygen-consuming photodynamic therapy to achieve further improved treatment efficacy [29-30].

In this work, we ought to combine glucose-consuming starvation therapy with the combination of hypoxia-activated prodrugs for synergistic cancer treatment. Glucose oxidase (GOx), a widely used enzyme in food industry, which can convert glucose, oxygen and water into gluconic acid and H_2O_2 [10, 11, 31-35], is encapsulated inside polyethylene glycol (PEG) modified stealth liposomes as a glucose and oxygen depletion agent (**Figure 1a**). It is found that the high tumor accumulation of liposome-GOx with long blood half-life would contribute to effective tumor oxygen depletion to enhance tumor hypoxia and consume glucose at short time post intravenous (i.v.) injection. Apart from consumption of glucose and oxygen, GOx also increases the intratumoral oxidative stress that can induce cell apoptosis by producing a high level of H_2O_2, as evidenced by *in vivo* photoacoustic imaging using a H_2O_2-specific probe [10, 36]. Thereafter, a hypoxia-activated prodrug, AQ4N, is also encapsulated inside PEGylated liposome for the subsequent tumor-targeted delivery to induce further cancer cell damages [29, 37, 38]. Notably, the combination of starvation therapy and hypoxia-activated therapy with co-administration of liposome-GOx and liposome-AQ4N leads to highly effective tumor growth inhibition in the mouse tumor model experiment. Without significant toxic side effects, such combination therapy delivered by liposomes formulated with biocompatible components may be a promising strategy for next generation cancer therapy.

2. **Materials and experiments**

2.1 Materials

Glucose oxidase (GOx, 100 units/mg protein) was purchased from Sigma-Aldrich. AQ4N was purchased from Abcam. Dipalmitoylphosphatidylcholine (DPPC), PEG_{5k} conjugated distearinphosphatidylethanolamine ($DSPE\text{-}mPEG_{5k}$) and cholesterol were purchased from Xi'an Ruixi Biological Technology Co., Ltd., Laysan Bio Inc. and *J&K* Scientific Ltd, respectively. 1,1'-dioctadecyl-3,3,3',3'-tetramethylindodicarbocyanine perchlorate (DiD) and 1,1'-dioctadecyl-3,3,3',3'-tetramethylindotricarbocyanine iodide (DiR) were purchased from AAT Bioquest, Inc. 3-(4,5-dimethylthiazol-2-yl)-2,5-diphenyl-tetrazolium bromide (MTT) was purchased from Sigma-Aldrich. Glucose-free Roswell Park Memorial Institute (RPMI)-1640 medium, normal RPMI-1640 medium, Dulbecco's Modification of Eagle's Medium (DMEM) and fetal bovine serum (FBS) were purchased from Thermo Fisher Scientific Inc.

2.2 Liposome preparation

To prepare liposome-GOx and liposome-AQ4N, the lipid mixture of DPPC, cholesterol and $DSPE\text{-}mPEG_{5k}$ were dissolved into chloroform at a mole ratio of 8 : 4 : 1. Then the lipid solution was dried under vacuum. After that, the obtained lipid was hydrated with AQ4N or GOx solution (10 mg mL^{-1} for AQ4N, 8 mg mL^{-1} for GOx) and stirred under 45 ^{o}C for 30 min, followed with being extruded through a 200 nm polycarbonate filter for 20 times. The excess GOx and AQ4N were removed by using Sephacryl S-300 high resolution column (GE Healthcare) and Sephadex G-100 (Sigma), respectively. To prepare liposome-GOx-DiR/DiD and liposome-AQ4N-DiR, the lipid membranes consisting of DPPC, cholesterol, $DSPE\text{-}mPEG_{5k}$ and DiR/DiD at a mole ratio of 8 : 4 : 1 : 1 were firstly prepared, and then hydrated, extruded and separated via the aforementioned

procedure. The preparation of liposome-HRP-ABTS followed the method in a recent work of our group [39].

2.3 Liposome characterization

The dynamic light scattering (DLS) measurement was carried out with a Malvern Zetasizer (Nano Z90). The morphology was observed under a Tecnai Cryo-TEM (FEI, Hillsboro, OP) at an accelerating voltage of 120 kV. The absorbance of liposome-GOx and liposome-AQ4N were detected by a UV-vis-NIR spectrometer (Genesys 10S, Thermo). The concentration of AQ4N was calculated from the absorbance at 610 nm with mass extinction coefficient of 22.5 mL mg^{-1} cm^{-1}. The concentration of GOx was measured by using the standard bicinchoninic acid (BCA) protein assay (Thermo Scientific).

2.4 Catalytic ability measurement

To measure the catalytic ability of liposome-GOx, different concentrations of glucose solutions were treated with liposome-GOx or free GOx (10 μg mL^{-1}) with continuous oxygen supply at a concentration of ~9 mg L^{-1} by oxygen bubbling. At different time points, the solutions were collected to detect H_2O_2 and pH. The pH value was measured by a pH meter (FE28, METTLER TOLEDO). The concentration of H_2O_2 was measured by adding $TiOSO_4$ (0.03 mol L^{-1}) that would react with H_2O_2 to form stable primrose yellow complexes. The absorbance of each sample at 405

nm was measured with a UV-vis spectrometer to calculate the concentration of H_2O_2 by comparing with the standard calibration curve obtained by H_2O_2 solutions with known concentrations.

2.5 Cell experiments

4T1 murine breast cancer cells, NIH 3T3 mouse embryonic fibroblast cells and RAW 264.7 murine macrophage cells were brought from the American Type Culture Collection (ATCC). According to the recommended procedure, 4T1 cells were cultured in RPMI-1640 medium supplemented with 10% FBS and 1% penicillin/streptomycin under humidified normoxic (95% air, 5% CO_2) conditions at 37 ^oC, while the other two types of cells were cultured in DMEM cell culture medium supplemented with 10% FBS and 1% penicillin/streptomycin under the same condition.

To evaluate cell cytotoxicity of liposome-GOx, 4T1 cells pre-seeded in 96 well plates with glucose-free RPMI-1640 cell culture medium were incubated with different concentrations of liposome-GOx, in the absence or presence of added glucose for 24 h, before the standard MTT assay. NIH 3T3 fibroblast cells and RAW 264.7 macrophage cells were pre-seeded in 96 well plates for 4 h before being treated with different concentrations of liposome-GOx (glucose: 1 mg mL^{-1}) for another 24 h. After that, the cell viability was measured using the standard MTT assay as aforementioned. To measure the hypoxia-activated cytotoxicity of liposome-AQ4N, 4T1 cells pre-seeded in 96-well plates were incubated with different concentrations of liposome-AQ4N under hypoxic (1% O_2, 5% CO_2 balanced with N_2) or normoxic (95% air, 5% CO_2) conditions for 48 h, before the standard MTT assay.

To measure the intracellular H_2O_2 concentration in 4T1 cells after being treated with liposome-GOx, cells pre-seeded in 12 well plates with glucose-free RPMI-1640 medium were incubated with different concentrations of liposome-GOx and fixed glucose concentration (100 μg mL^{-1}) for 6 h. Then, these cells were harvested and collected by centrifugation, followed by being dispersed with acetone (1 mL for each well) in an ice bath. After that, the acetone solutions were centrifuged to collect the supernatant at 14800 rpm for 5 min. Afterwards, 100 μL $TiOSO_4$ (0.03 mol L^{-1}) and 200 μL $NH_3 \cdot H_2O$ (~28%) were added into each supernatant to form yellow titanium peroxide complex ($Ti(IV)O_2^{2+}$) precipitation, which was collected by centrifugation at 14800 rpm for 5 min and re-dissolved in 1 mL H_2SO_4 solutions (1 mol L^{-1}). The concentrations of H_2O_2 were calculated by recording the absorbance of the yellow solution at 405 nm using a UV-Vis spectrophotometer.

To detect the cellular uptake of liposome-GOx-DiD, 4T1 cells pre-cultured with glucose-free RPMI-1640 medium was incubated with liposome-GOx-DiD (GOx, 25 μg mL^{-1}) containing medium for 2 h. Then, cells were washed by phosphate buffered saline (PBS) for 3 times and stained by the Lyso-tracker Green (Invitrogen) following the vendor's protocol. Finally, the cells were stained with 4, 6-diamino-2-phenylindole (DAPI) and observed under the confocal laser scan microscopy (CLSM, Leica TCS-SP5II, Germany).

To study the intracellular distribution of liposome-AQ4N, 4T1 cells were cultured in 12 well plates under normoxic condition (95% air, 5% CO_2) for 24 h. Then, the fresh culture medium containing liposome-AQ4N (AQ4N, 2 μM) was added into cells for another 8 h treatment under hypoxic (1% O_2, 5% CO_2 balanced with N_2) or normoxic condition (95% air, 5% CO_2). Afterwards, cells were washed with PBS and stained by Lyso-tracker Green and DPAI for CLSM observation.

To ensure the fluorescences enhancement of liposome-AQ4N in 4T1 cells under hypoxic culture environment, the 4T1 cells were seeded in 24 well plates under normoxic condition for 24 h. Afterwards, liposome-AQ4N (AQ4N, 2 μM) and liposome-DiD (DiD, 1 μM) were added into culture medium under hypoxic or normoxic condition for 8 h. Then, cells were collected and washed with PBS containing 1 % FBS for standard flow cytometry measurement (Calibur FACS instrument, BD).

2.6 Tumor model

6~8 weeks female balb/c nude mice were obtained from Nanjing Sikerui Biological Technology Co. Ltd. and used under protocols approved by the laboratory animal center of Soochow University. To build the 4T1 tumor model, 50 μL PBS containing ~2×10^6 4T1 cells was subcutaneously injected onto the back of each mouse.

2.7 Blood circulation measurement

To study the blood circulation profiles of liposome-GOx and liposome-AQ4N, mice were i.v. injected with DiR-labeled liposome-GOx-DiR or liposome-AQ4N-DiR (GOx: 2 mg kg^{-1}, AQ4N: 5 mg kg^{-1}, DiR: 2 mg kg^{-1}). Then, ~20 μL of blood was collected at each time interval post injection (p.i.), followed by being weighted and lysed with 1 mL lysis buffer (0.25 M sucrose, 40 mM tris-acetate, 10 mM ethylenediaminetetraacetic acid, EDTA) by sonication. After being centrifuged to remove the sediment, 100 μL solution of each sample was added into a 96 well black plates to

measure fluorescence intensity using a multimode microreader (Varioskan Flash, Thermo Fisher). The blood levels of DiR were presented as the percentage of the injected dose per gram tissue (%ID g^{-1}).

2.8 In vivo fluorescence imaging

For in vivo fluorescence imaging, 4T1 tumor bearing mice were i.v. injected with liposome-AQ4N-DiR, liposome-GOx-DiR, or liposome-AQ4N-DiR plus liposome-GOx (GOx: 2 mg kg^{-1}, AQ4N: 5 mg kg^{-1}, DiR: 2 mg kg^{-1}) for *in vivo* fluorescence imaging under the IVIS® *in vivo* optical imaging system (Lumina III, PerkinElmer, Inc.) at different time intervals. After 24 h, the major mouse organs were collected for *ex vivo* fluorescence imaging by the same imaging system. The statistics of fluorescence intensity was calculated based on the readouts of the auto-analysis software provided by the manufacturer.

2.9 In vivo photoacoustic (PA) imaging

For PA imaging of tumoral oxygenation levels, 4T1 tumor bearing mice were divided into two groups with either saline or liposome-GOx injection (GOx, 1 mg kg^{-1}). The mice were placed on the PA imaging equipment (Visualsonic Vevo® 2100 LAZER) for tumor blood oxygen detection at different time intervals p.i., using the Oxy-Hemo mode according the standard protocol [40].

To detect the H_2O_2 levels in the tumor, the liposome-HRP-ABTS were synthesized as a H_2O_2-specific PA imaging probe following our reported protocol [39]. 4T1 tumor bearing mice

were divided into 3 groups: 1, saline injection; 2, liposome-HRP-ABTS injection; 3, liposome-GOx and liposome-HRP-ABTS co-injection. The doses of horseradish peroxidase (HRP), 2, 2'-azino-bis(3-ethylbenzothiazoline-6-sulfonic acid (ABTS) and GOx were 7.4, 34.5, and 1 mg kg^{-1}, respectively. The PA signals of tumors in different groups at 800 nm were recorded at different time intervals p.i.

2.10 Ex vivo immunofluorescence staining

4T1 tumor bearing mice with i.v. injection of liposome-GOx (GOx, 2 mg kg^{-1}) were scarified at 12 h or 24 h post injection for frozen section and immunofluorescence staining. The hypoxia staining was carried out using Hypoxyprobe-1 plus kit (Hypoxyprobe Inc.) following the reported protocol [22]. HIF-1α staining was carried out using anti-HIF-1α antibody following the vendor's protocol. Blood vessels and cell nuclei were stained by anti-CD31 antibody and DAPI, respectively. All immunofluorescence staining assays were carried out following standard procedures. All tumor sections were imaged under CLSM. The statistical data of hypoxia/ HIF-1α signals were obtained by ImageJ software, with more than 10 slices analyzed per group.

2.11 In vivo combination cancer therapy

A total of 25 4T1-tumor-bearing female Balb/c nude mice were divided into 5 groups: I) control group with PBS injection only; II) i.v. injection of liposome-AQ4N; III) i.v. injection of liposome-GOx; IV) i.v. injection of free GOx and AQ4N; V) i.v. injection of liposome-GOx and liposome-AQ4N. The doses of AQ4N and GOx were 5 and 2 mg kg^{-1}, respectively. When the tumor volume reached ~100 mm^3, the mice received three times of injections with different agents at day

0, 4 and 8. Since day 0, the tumor width and length were recorded using a digital caliper. The tumor volume was calculated based on an equation of volume = width^2 × length/2 for drawing tumor growth curves. A tumor of each group was collected by surgical resection after 48 h post the first treatment for fluorescence terminal deoxynucleotidyl transferase-mediated dUTP-biotin nick end labeling (TUNEL) staining by following the vendor's protocol. After treatment at day 14, all the mice were executed and their organs were collected for hematoxylin and eosin (H&E) staining.

3. Results and Discussion

Liposome, as a mature and eminent nanomedicine carrier with great biocompatibility, preeminent pharmacokinetic profiles as well as multiple drug loading abilities, has been approved for clinical use as therapeutics carriers (*e.g.* Doxil, DaunoXome) [41, 42]. In this work, the GOx enzyme and the small molecule hypoxia-activated prodrug AQ4N were encapsulated into PEGylated liposomes separately for combination of starvation and hypoxia-activated therapy (**Figure 1a**). After careful optimization, liposome-AQ4N and liposome-GOx were obtained following the standard liposome synthesis method by hydrating lipid films consisting the mixture of DPPC, cholesterol and DSPE-mPEG$_{5k}$ at the molar ratio of 8 : 4 : 1, with an aqueous solutions of GOx or AQ4N, respectively. Although liposomes with co-loading of AQ4N and GOx could also be prepared, our preliminary results indicated that loading of GOx into liposomes could significantly reduce the loading efficiency of AQ4N.

As observed under Cryo-transmission electron microscopy (Cryo-TEM), both liposome-GOx and liposome-AQ4N exhibited spherical-like structure with average sizes of ~100 nm (**Supporting**

Figure S1). From the dynamic light scattering (DLS), we found the hydrodynamic diameter of liposome-GOx to be ~140 nm, which was slightly larger than that of liposome-AQ4N at ~100 nm (**Figure 1b**). After removal of excess GOx and AQ4N using size-exclusion separation columns, the loading efficiencies of GOx and AQ4N were determined to be 5% and 10% as measured by the standard bicinchoninic acid (BCA) protein assay or UV-vis-NIR absorbance spectra, respectively. By incubating free GOx and liposome-GOx (GOx = 10 μg mL^{-1}) with glucose solution under enough O_2 supply, quickly decreased pH and increased H_2O_2 concentration within the mixed solutions were observed, indicating that GOx within liposome-GOx could effectively catalyze the conversion of glucose, H_2O and O_2 into gluconic acid and H_2O_2, without obvious catalytic ability lose compared with free GOx (**Figure 1c&d, Supporting Figure S2**).

Then, the *in vitro* behaviors of liposome-GOx were studied by a series of cell experiments. To facilitate *in vitro* tracking, DiD, a lipophilic fluorescent dye, was used to label liposomes. 4T1 murine breast cancer cells were incubated with such liposome-GOx-DiD for CLSM observation to study the cellular internalization of those enzyme-loaded liposomal nanoparticles. The co-localized DiD fluorescence with lysosomes stained with Lyso-Tracker suggested the cellular uptake of those liposomal nanoparticles likely via endocytosis (**Figure 2a**). Next, the cytotoxicity of liposome-GOx was measured by the standard MTT cell viability assay. It was found that the liposome-GOx had no obvious toxicity to 4T1 cells within a glucose-free cell culture medium (**Figure 2b**). In contrast, in the presence of glucose, liposome-GOx showed increased toxicity to cells with increasing concentrations of glucose and GOx (**Figure 2b**). Apart from showing great toxicity to 4T1 breast cancer cells, such liposome-GOx exhibited significant concentration dependent toxicity to non-cancer cells (*e.g.* NIH 3T3 fibroblast cells and RAW 264.7 macrophage cells, **Supporting**

Figure S3). We further measured the H_2O_2 concentration in cells after being incubated with liposome-GOx and glucose for 6 hours. The increasing concentrations of intracellular H_2O_2 were observed, indicating that such liposome-GOx would induce prominent cell toxicity mainly by catalyzing glucose to produce abundant H_2O_2, which would then impose severe oxidative stress to both tumor cells and those stroma cells (**Figure 2c**).

In the active metabolism of AQ4N, low toxic AQ4N would be reduced to AQ4, a DNA-affiliative intercalator/topoisomerase II toxicant, by a series of specific reductase (*e.g.* cytochrome P450, nitric oxide synthase) only under hypoxic microenvironment [37]. Hence, we carefully studied the intracellular behaviors of liposome-AQ4N. Firstly, the intracellular distribution of liposome-AQ4N was imaged by CLSM. Interestingly, compared to 4T1 cells incubated with liposome-AQ4N under the normoxia condition, stronger fluorescence signals of AQ4N were observed in cells incubated with liposome-AQ4N under the hypoxia condition, with fluorescence signals noted even inside cell nuclei (**Figure 2d**). However, if we used DiD to track the cellular behaviors of liposomes, it was found that the cellular uptake of liposomes themselves showed little difference between hypoxia and normoxia conditions, indicating that the hypoxia-enhanced AQ4N fluorescence might be attributed to the drug release and metabolism under hypoxic environment (**Supporting Figure S4**). Such phenomena suggest that AQ4N after cellular uptake under hypoxia environment would be released from liposome and reduced into hydrophobic AQ4, which would then be able to diffuse across lysosome membrane into cytoplasm and then enter cell nuclei to integrate with nuclear DNA [43]. Following that, the cytotoxicity of liposome-AQ4N under normoxia/hypoxia conditions was determined by the MTT assay. As expected, liposome-AQ4N exerted obvious hypoxia-selective cell toxicity (**Figure 2e**).

Next, we carefully studied the in vivo performance of liposome-GOx and liposome-AQ4N after i.v. injection into 4T1 tumor bearing mice. The liposome-GOx and liposome-AQ4N were both labeled with DiR, a lipophilic near infrared (NIR) fluorescent dye, to facilitate *in vivo* tracking [29]. By collecting blood samples at different time intervals after i.v. injection of liposome-GOx-DiR or liposome-AQ4N-DiR, the blood circulation curves of the two types of liposomes were determined. It was found that both liposome-GOx and liposome-AQ4N had long blood half-lives (liposome-GOx: $t_{1/2\alpha}$ = 1.65 ± 0.06 h, $t_{1/2\beta}$ = 10.93 ± 1.43 h; liposome-AQ4N: $t_{1/2\alpha}$ = 2.4 ± 0.96 h, $t_{1/2\beta}$ = 10.08 ± 3.53 h) (**Figure 3a**). At the same time, those mice were imaged by an *in vivo* fluorescence imaging system. The time-dependent increased fluorescence signals at the tumor site indicated the efficient tumor homing of both liposome-GOx-DiR and liposome-AQ4N-DiR, by the enhanced permeability and retention (EPR) effect owing to the unique abnormal vasculature and lack of effective lymph drainage in tumors (**Figure 3b**). After 24 h of both injections, the main organs of mice were collected to observe their detailed biodistribution profiles. The tumor fluorescence signals of the two groups were both obviously stronger than that in the liver, not to mention the other organs, further confirming the great tumor accumulation abilities of both liposome-GOx-DiR and liposome-AQ4N-DiR (**Figure 3c&d**). Moreover, it was interesting to find that the concomitant injection of liposome-AQ4N-DiR plus liposome-GOx showed similar *in vivo* pharmacokinetic profiles to that of liposome-AQ4N-DiR injected alone, under the tested doses (**Supporting Figure S5**).

After affirming the tumor accumulation, we studied the intratumoral hypoxia status and H_2O_2 production of those mice after starvation therapy with liposome-GOx by employing the non-invasive PA imaging technique, an efficient testing method for intratumoral blood oxygen

levels and nanomaterials accumulation (**Figure 4a**) [40, 44]. By means of the Oxy-Hemo mode of the PA imaging system, by recording the PA signal of de-oxygenated hemoglobin at 750 nm and oxygenated hemoglobin at 850 nm, we observed that the tumor blood oxygen level (sO_2 Average) of mice showed ~80% dropping within 2 h post i.v. injection of liposome-GOx, while the control group showed no significant change (**Figure 4b&c**). However, such liposome-GOx injection showed minimal influence on the blood oxygen levels of healthy organs (*e.g.* legs) under the same treatment protocol as aforementioned (**Supporting Figure S6**). Those results indicate that i.v. injection of liposome-GOx would efficiently and specifically exhaust the intratumoral oxygen, leading to significantly enhanced tumor hypoxia without obviously impairing those healthy organs / tissues.

In our recent work, a unique type of H_2O_2-specific PA imaging probe was developed by encapsulating both HRP and ABTS into PEGylated liposomes. In the presence of H_2O_2, the colorless ABTS within liposome-HRP-ABTS could be oxidized into bluish product as catalyzed by HRP (**Figure 4a**), generating strong NIR absorbance and thus high contrast capacity under PA imaging (**Supporting Figure S7**) [39]. Therefore, liposome-HRP-ABTS was applied to detect the H_2O_2 produced within the tumor after i.v. injection of liposome-GOx. In our experiments, liposome-HRP-ABTS was co-injected with liposome-GOx into 4T1 tumor bearing mice for real-time detection of intratumoral H_2O_2 generation under PA imaging at 800 nm excitation. Compared to tumors on control mice, those on mice injected with liposome-HRP-ABTS, regardless of liposome-GOx injection, showed increased H_2O_2-specific PA signals at 1 h post injection, suggesting the existence of endogenous H_2O_2 within the tumor microenvironment (**Figure 4d&e**). Interestingly, at 2 h post injection of liposome-HRP-ABTS, the H_2O_2-specific PA signals in tumors

for mice treated with liposome-GOx appeared to be obviously stronger than that without liposome-GOx treatment, demonstrating that the intratumoral H_2O_2 level was further increased by i.v. injection of liposome-GOx. Therefore, our PA imaging results clearly illustrate that GOx delivered into tumors by liposomes could indeed trigger the oxidization of glucose to produce extra H_2O_2, which would increase the oxidative stresses of tumor cells.

Following that, to further ensure the enhanced tumor hypoxia induced by liposome-GOx over longer term, *ex vivo* immunofluorescence staining of tumor slices with both exogenous pimonidazole probe and hypoxia induced factor 1α (HIF-1α) as a endogenous marker was implemented. After i.v. injection of liposome-GOx (GOx: 2 mg kg^{-1}) for 12 h or 24 h, the tumors were collected from mice and freezing sectioned for immunofluorescent staining following the standard protocol [22]. It was found that both pimonidazole signals and HIF-1α positive signals were obviously increased for tumor slices with i.v. injection of liposome-GOx, clearly evidencing the tumor hypoxia status was dramatically enhanced over a relatively long period of time (**Figure 5a&b, Supporting Figure S8**). The enhancement of hypoxia by liposome-GOx indicates the effective consumption of glucose and oxygen within the tumor by the starvation therapy to cut down the tumor energy supply, and moreover, simultaneously creating suitable tumor microenvironment for hypoxia-activated therapy.

Finally, the *in vivo* synergistic therapeutic effect of liposome-GOx and liposome-AQ4N were evaluated using the 4T1 mouse tumor model. A total of 25 mice bearing 4T1 tumors were divided into five groups: I) control group with PBS injection； II）liposome-GOx injection; III) liposome-AQ4N injection; IV) free GOx + free AQ4N injection; V) liposome-GOx + liposome-AQ4N injection. The treatment doses of GOx and AQ4N for one injection were 2 and 5

mg kg^{-1}, respectively, for the correlated groups. All mice were treated three times on day 0, 4, and 8 by i.v. injection of various agents. The tumor sizes were recorded for 16 days, by then tumors were collected and weighted (**Figure 5c&d**). It was found that the mice received co-injection of liposome-GOx and liposome-AQ4N gained the best tumor inhibition effect, in comparison to all other groups. Although hypoxia-activated therapy by liposome-AQ4N could also partly delay the tumor growth, its tumor inhibition efficacy was obviously lower compared to that achieved with combination therapy. On the other hand, we found that i.v. injection of liposome-GOx itself could only slightly inhibit the tumor growth, suggesting that the antitumor efficacy of starvation therapy alone at our used dose was still limited. Moreover, the therapeutic efficacy achieved with the combination use of free AQ4N and free GOx was also not significant, likely owing to their limited tumor retention in the free forms.

To further evaluate the combined treatment efficacy, the TUNEL staining was carried out for tumors of mice two days after the first injection (**Figure 5e**). The highest TUNEL signals were observed in the group V with the combination treatment by both liposome-GOx and liposome-AQ4N. Moreover, as examined by histological examination (**Supporting Figure S9**), the combination treatment with liposome-GOx and liposome-AQ4N showed no obvious acute toxicity to the treated animals. Given that the liposome-GOx injection showed minimal influence on the blood oxygen levels of those healthy organs / tissue, we thus conclude that the combination of starvation therapy with hypoxia-activated therapy by delivering both GOx and AQ4N into tumors with liposomal carriers could be an effective approach for cancer treatment.

4. Conclusion

In summary, we designed an innovative cancer treatment strategy by combining GOx-based starvation therapy and AQ4N-based hypoxia-activated therapy using liposomal nanocarriers. After being encapsulated in long-circulating stealth liposomes, GOx and AQ4N could be sequentially delivered to tumors with high tumor homing efficiencies. As illustrated by *in vivo* PA imaging, such liposome-GOx could specifically block tumorous glucose supply, exhaust tumorous oxygen for hypoxia enhancement, and produce toxic H_2O_2 inside the tumors. In the meanwhile, liposome-AQ4N once inside the tumor with enhanced hypoxia would be further activated to achieve strong synergistic antitumor effect. Our work thus presents a rather simple approach to combine starvation therapy with hypoxia-activated therapy using the well-established liposomal systems to achieve an obvious synergistic therapeutic outcome. As all agents involved in our system are biodegradable ones, such a new cancer treatment strategy may bring new thinking for cancer treatment research, even promising for clinical translation.

Acknowledgements

This work was partially supported by the National Research Programs from Ministry of Science and Technology (MOST) of China (2016YFA0201200), the National Natural Science Foundation of China (51525203, 51761145041), the China Postdoctoral Science Foundation (2017M610348), Collaborative Innovation Center of Suzhou Nano Science and Technology, the 111 Program from the Ministry of Education of China, and a Project Funded by the Priority Academic Program Development (PAPD) of Jiangsu Higher Education Institutions.

Supporting Information. Supplementary data related to this article can be found at …

Supplementary Figures S1-S9. (PDF)

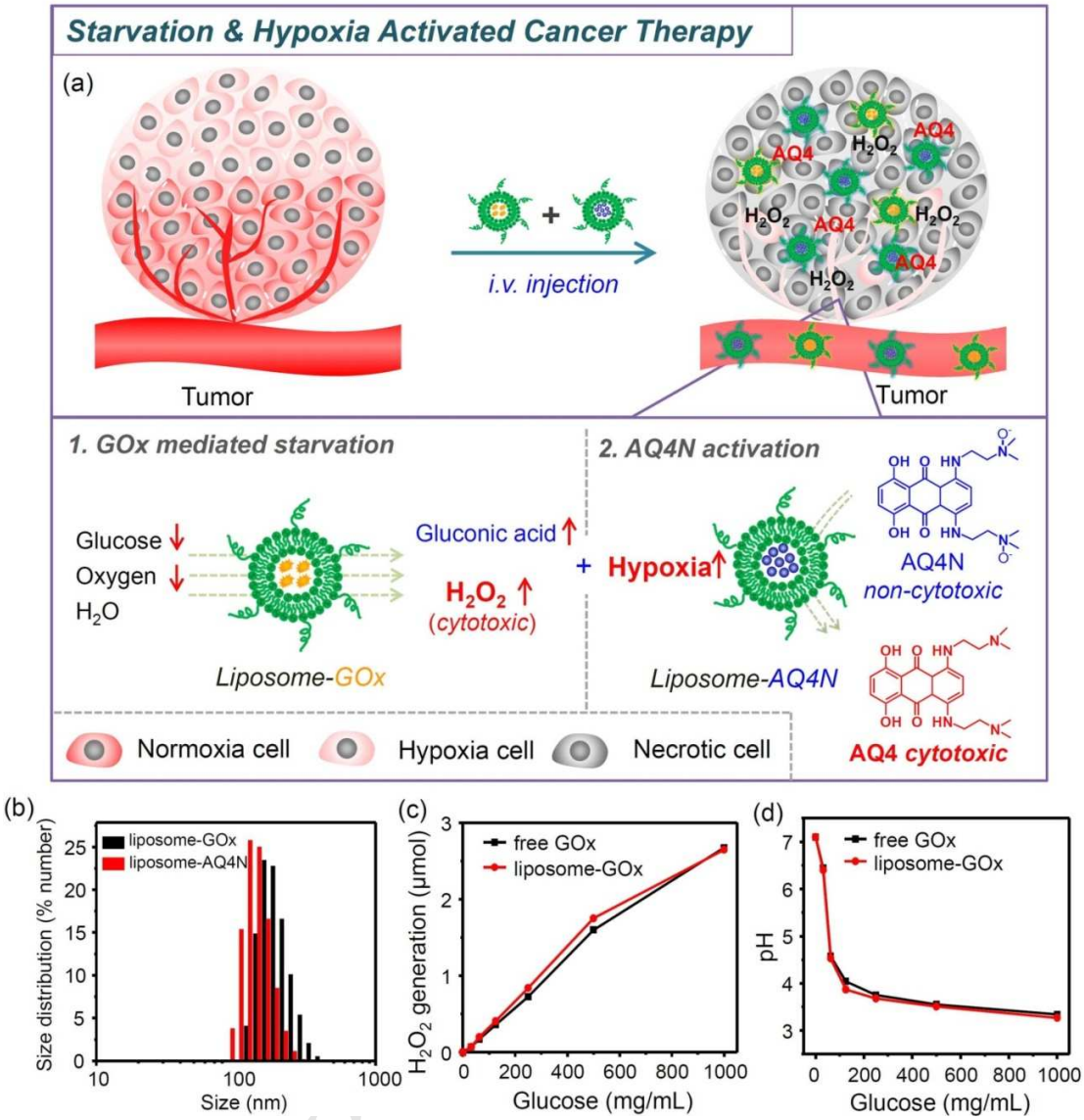

Figure 1. Scheme of experimental design and characterization of liposomes. **(a)** A scheme illustrating the design of combining starvation and hypoxia-activated therapy by co-delivery of liposome-GOx and liposome-AQ4N into tumors. (b) DLS size distributions of liposome-AQ4N and liposome-GOx. (c) The generated H_2O_2 levels in glucose solutions at different concentrations after adding liposome-GOx or free GOx. (d) Changes of pH values in glucose solutions with different concentrations after adding liposome-GOx or free GOx.

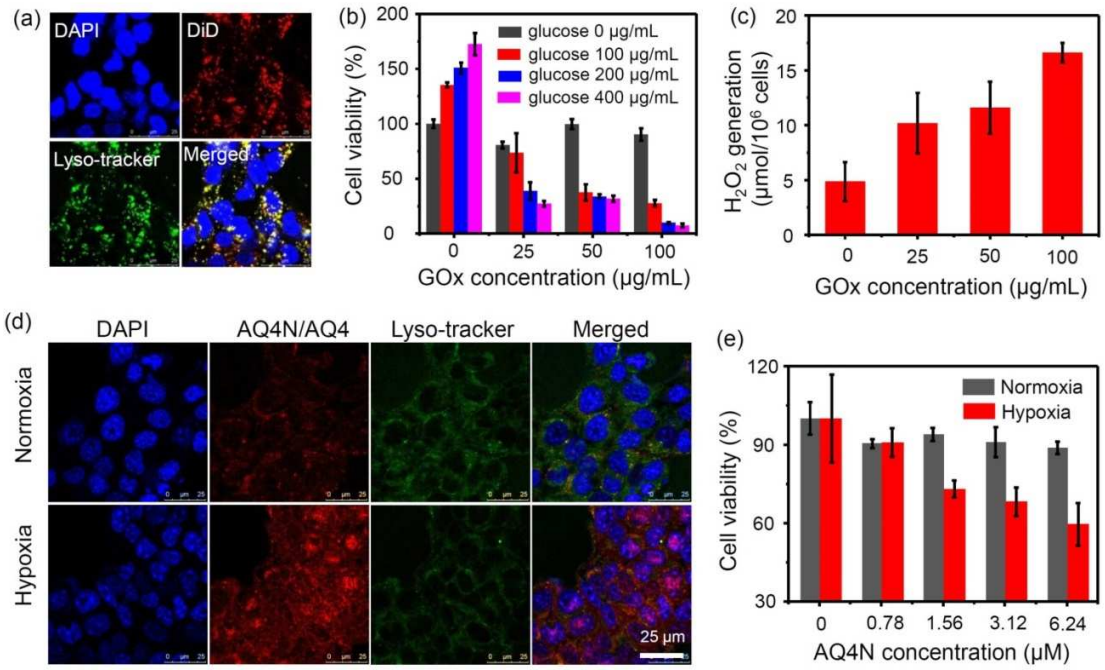

Figure 2. In vitro behaviors of liposome-GOx and liposome-AQ4N. (a) Confocal fluorescence images of 4T1 cells after incubation with liposome-GOx-DiD. (b) Relative viabilities of 4T1 cells after 24 h incubated with different concentrations of glucose and liposome-GOx. (c) H_2O_2 generation in 4T1 cells (10^6 cells) after incubation with different concentrations of liposome-GOx for 6 h, in the presence of 100 μg/mL glucose. (d) Confocal fluorescence images of 4T1 cells after incubation with liposome-AQ4N (10 μM) for 12 h, under the normoxia or hypoxia culture condition. (e) Relative viabilities of 4T1 cells after 48 h incubation with different concentrations of liposome-AQ4N under the normoxia or hypoxia culture condition.

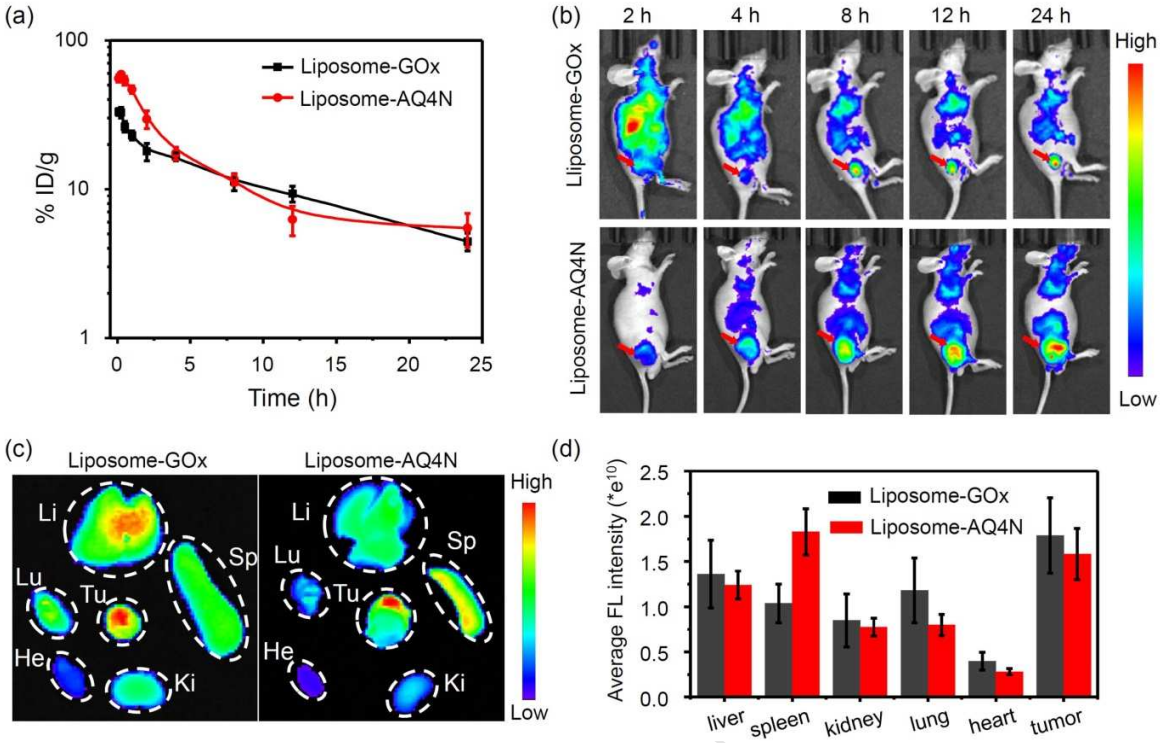

Figure 3. In vivo behaviors of liposome-GOx and liposome-AQ4N. (a) Blood circulation curves of liposome-GOx-DiR and liposome-AQ4N-DiR by measuring the DiR fluorescence in the blood at different time points post-injection. (b) Time-lapsed in vivo fluorescence images of 4T1 tumor-bearing mice with i.v. injection of liposome-GOx-DiR or liposome-AQ4N-DiR. The tumors were indicated with arrows in red. (c) Ex vivo fluorescence imaging of main organs/tissues from mice after i.v. injection of liposome-GOx-DiR or liposome-AQ4N-DiR for 24 h. Li, Sp, Ki, He, Lu, and Tu stand for liver, spleen, kidney, heart, lung and tumor, respectively. (d) Semi-quantitative analysis of fluorescence signals of each organ / tissue based on the images shown in (c).

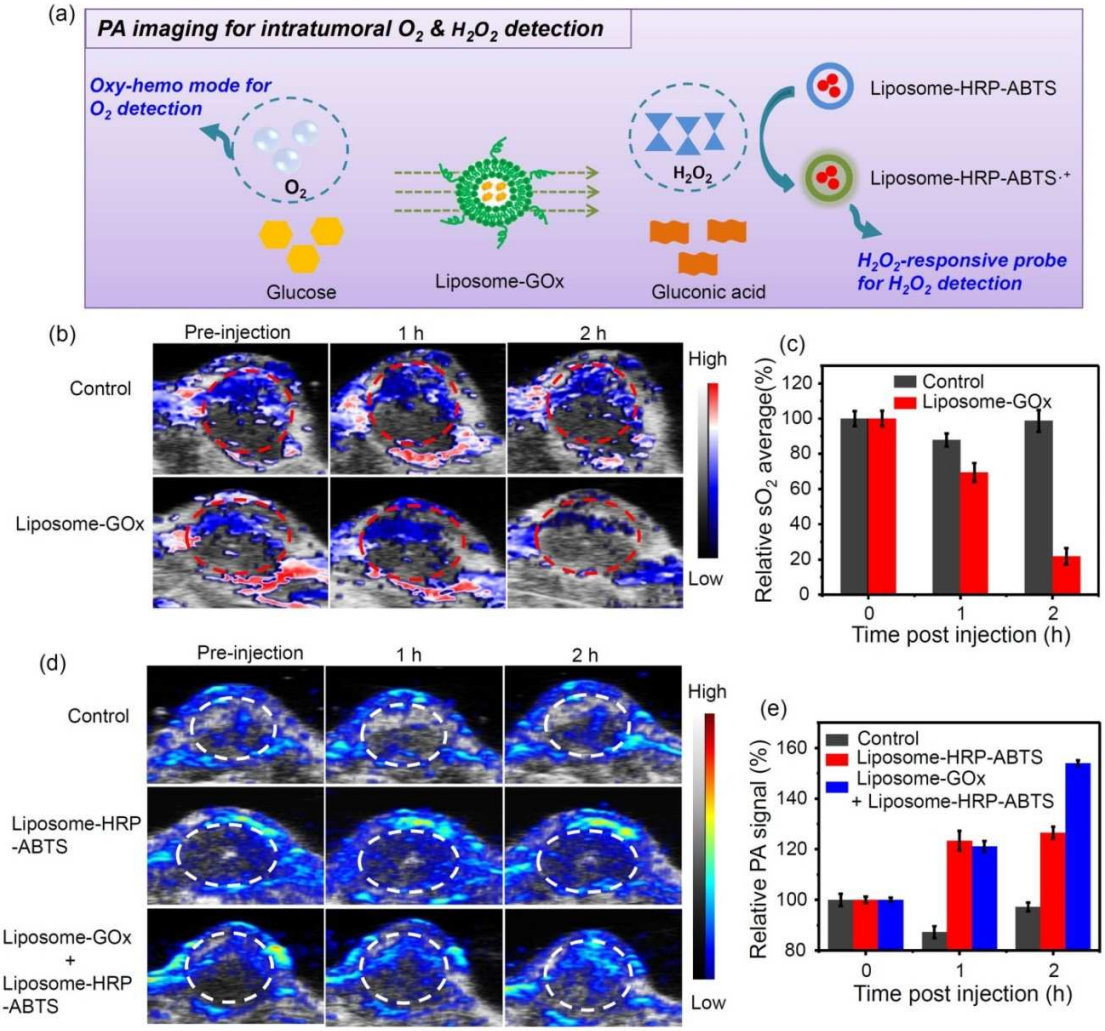

Figure 4. Tumor hypoxia and H_2O_2 detection after injection of liposome-GOx by in vivo PA imaging. (a) A scheme of PA imaging of intratumoral O_2 and H_2O_2. (b) PA images of 4T1 tumor blood oxygen saturation (sO_2) levels before or at different time intervals after i.v. injection of liposome-GOx or saline. The color scale was calculated from the PA signal ratios between de-oxygenated (750 nm) and oxygenated hemoglobin (850 nm). The grey scale was B-mode ultrasound signals. (c) Quantification of sO_2 average total signals in (b). (d) PA images of 4T1 tumors to detect intratumoral H_2O_2 by the liposome-HRP-ABTS nanoprobe, without or with co-injection of liposome-GOx. (e) Quantification of H_2O_2-induced PA signals for tumors in (d).

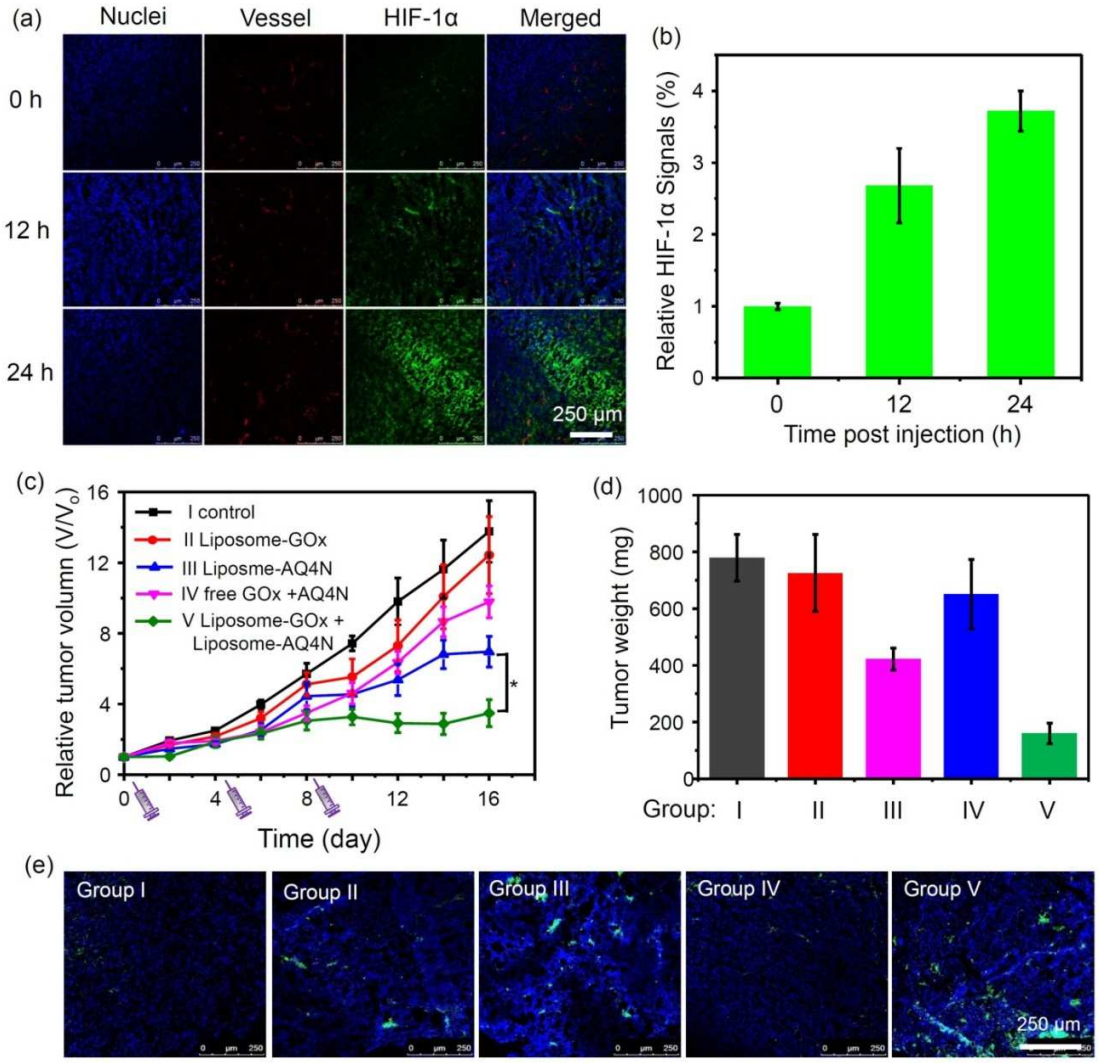

Figure 5. In vivo starvation and hypoxia-activated therapy. (a) Ex vivo immunofluorescence staining of HIF-1α for tumor slices collected from mice before (0 h) and after injection of liposome-GOx at 12 h and 24 h. The cell nuclei, blood vessels, and HIF-1α were stained with DAPI (blue), anti-CD31 antibody (red) and HIF-1α antibody (green), respectively. (b) Quantification of HIF-1α positive areas based on the images shown in (a) by the Image J software (n = 10 images per tumor). (c) Tumor growth curves of mice after various different treatments indicated. The mice were divided into 5 groups: I) control; II) liposome-GOx; III) liposome-AQ4N; IV) free GOx and free AQ4N; V) liposome-GOx and liposome-AQ4N. All mice received 3 repeated injections at day 0, 4 and 8. (d) Average tumor weights of 5 groups of mice after different treatments collected at day 16. (e) Micrographs of TUNEL stained tumor slices collected from mice of different groups at day 2.